Chapter 2

Slip effects on MHD peristaltic transport of a Williamson fluid through a porous medium in a symmetric channel

2.1 Introduction

Peristaltic transport is a well known process of a fluid transport which is induced by a progressive wave of area contraction or expansion along the length of distensible tube containing the fluid. It is used by many systems in the living body to propel or to mix the contents of a tube. The peristalsis mechanism usually occur in urine transport from kidney to bladder, swallowing food through the esophagus, chyme motion in the gastrointestinal tract, vasomotion of small blood vessels and movement of spermatozoa in the human reproductive tract. There are many engineering processes as well in which peristaltic pumps are used to handle a wide range of fluids particularly in chemical and pharmaceutical industries. It is also used in sanitary fluid transport, blood pumps in heart lung machine, and transport of corrosive fluids, where the contact of the fluid with the machinery parts is prohibited. Because most of the physiological fluids behave like a non-Newtonian fluid, therefore, some interesting studies dealing with the flows of non-Newtonian fluids are given in (Bohme and Friedrich, 1983[11]; Siddiqui et al., 1991[52]; Hayat et al., 2002[24]; Srinivasacharya et al., 2003[56]; Subba Reddy et al., 2007[63], Nadeem and Akram, 2010[43]; Subba Reddy et al., 2011)[67].

Flow through a porous medium has been of significant interest in recent years particularly among geophysical fluid dynamicists. Examples of natural porous media are beach sand, sandstone, limestone, rye bread, wood, the human lung, bile duct, gall bladder with stones and in small blood vessels. Flow through porous medium has been studied by a number workers employing Darcy's law (Sceidgger, 1974[49]; Raptis and Perdikis, 1983[48]; Varshney, 1979[71]. Elshehawey and Husseny (2000)[19] have studied the peristaltic motion of a Newtonian fluid through a porous medium in a channel. The interaction of peristaltic flow with pulsatile fluid under the effect of a transverse magnetic field through a porous medium bounded by a two-dimensional channel is studied by Afifi and Gad (2001)[2]. Mekheimer and Arabi (2003)[40] studied

the non-linear peristaltic transport of MHD flow through a porous medium. Non-linear peristaltic transport through a porous medium in an inclined planar channel has studied by Mekheimer (2003)[39] taking the gravity effect on pumping characteristics. Vajravlu et al. (2007)[71] have investigated the peristaltic flow of a Newtonian fluid through a porous medium in a vertical annulus with heat transfer. Hall effects on peristaltic transport of a Maxwell fluid in a porous medium have been studied by Hayat et al. (2007)[31]. Subba Reddy et al. (2012)[[68] have investigated the non-linear peristaltic flow of a fourth grade fluid through a porous medium in an inclined asymmetric channel.

On the other hand it is observed that limited attention is paid to the peristaltic flows of non-Newtonian fluids when no-slip condition is not adequate. El Sehaway et al. (2006)[21] have studied the effect of slip on the peristaltic flow of a Maxwell fluid in a channel. The effects of slip and non- Newtonian parameters on the peristaltic flow of a third grade fluid in a circular cylindrical tube were investigated by Ali et al. (2009)[9]. Chaube et al. (2010)[12] have discussed the slip effects on the peristaltic flow of a micropolar fluid in a channel. Hayat et al. (2010)[35] have studied the simultaneous effects of partial slip and heat transfer on the peristaltic flow of viscous fluid in a two-dimensional channel are reported. Effect of slip and induced magnetic field on the peristaltic flow of pseudoplastic fluid was studied by Noreen et al. (2011)[46]. Subba Reddy et al. (2011)[66] have investigated the slip effects on the peristaltic motion of a Jeffrey fluid through a porous medium in an asymmetric channel under the effect of magnetic field.

In view of these, we studied the effects of slip and magnetic field on the peristaltic transport of a Williamson fluid through a porous medium in a two-dimensional channel under the assumptions of low Reynolds number and long wavelength. The flow is investigated in a wave frame of reference moving with velocity of the wave. The perturbation series in the Weissenberg number ($We < 1$) was used to obtain explicit forms for velocity field, pressure gradient per one wavelength. The effects of various pertinent parameters on the pressure gradient and pumping characteristics are discussed through graphs in detail.

This chapter was published in **J. Math. Comput. Sci. 3(5), 2013, 1306-1324**.

2.2 Mathematical Formulation

We consider the peristaltic transport of a Williamson fluid through a porous medium in a two-dimensional symmetric channel of width $2a$. The flow is generated by sinusoidal wave trains propagating with constant speed c along the channel walls. A uniform magnetic field B_0 is applied in the transverse direction to the flow. The fluid is taken to be of small electrical conductivity, so that the magnetic Reynolds number is small and the induced magnetic field is neglected in comparison with the applied magnetic field. Fig. 2.1 shows the physical model of the channel.

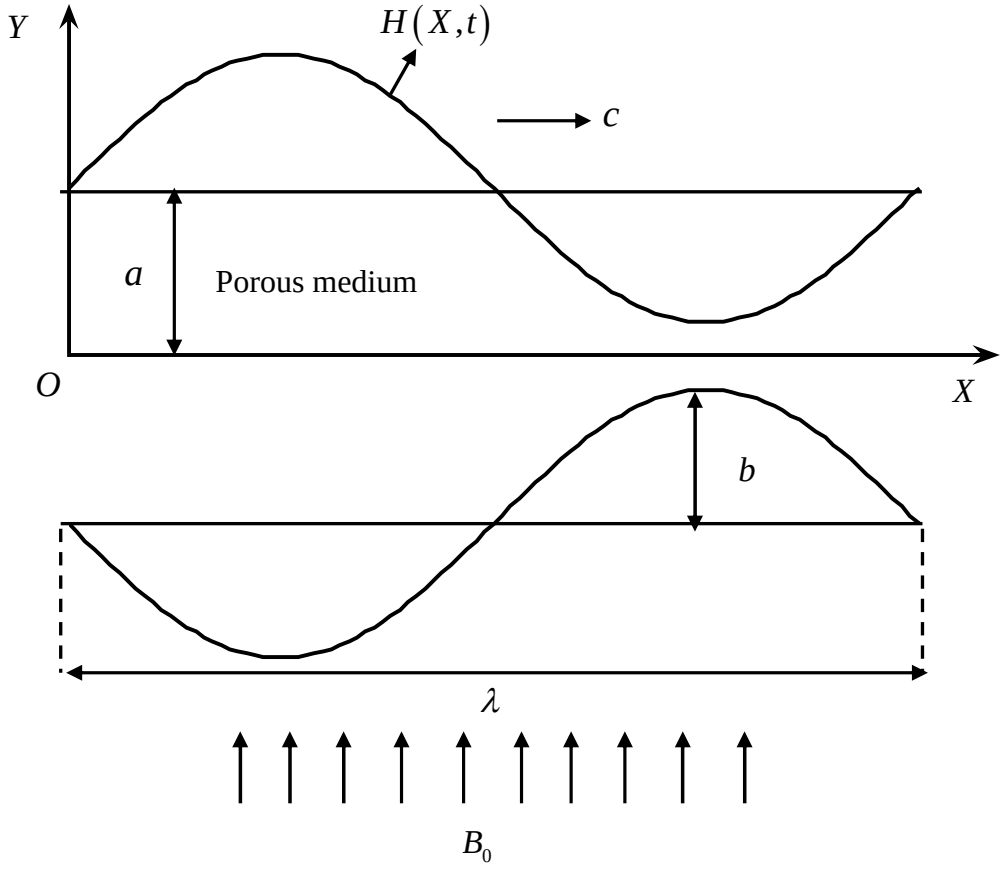

Fig. 2.1 The physical model

The wall deformation is given by

$$Y = \pm H(X,t) = \pm a \pm b\cos\frac{2\pi}{\lambda}(X - ct), \qquad (2.2.1)$$

where *b* is the amplitude of the wave, λ - the wave length and X and Y - the rectangular co-ordinates with X measured along the axis of the channel and Y perpendicular to X. Let (U,V) be the velocity components in fixed frame of reference (X,Y).

The flow is unsteady in the laboratory frame (X,Y). However, in a co-ordinate system moving with the propagation velocity c (wave frame (*x, y*)), the boundary shape is stationary. The transformation from fixed frame to wave frame is given by

$$x = X - ct, y = Y, u = U - c, v = V \tag{2.2.2}$$

where (u,v) and (U,V) are velocity components in the wave and laboratory frames respectively.

The constitutive equation for a Williamson fluid is

$$\tau = -\left[\eta_\infty + \left(\eta_0 + \eta_\infty\right)\left(1 - \Gamma\dot{\gamma}\right)^{-1}\right]\dot{\gamma} \tag{2.2.3}$$

where τ is the extra stress tensor, η_∞ is the infinite shear rate viscosity, η_o is the zero shear rate viscosity, Γ is the time constant and $\dot{\gamma}$ is defined as

$$\dot{\gamma} = \sqrt{\frac{1}{2}\sum_i\sum_j \dot{\gamma}_{ij}\dot{\gamma}_{ji}} = \sqrt{\frac{1}{2}\pi} \tag{2.2.4}$$

where π is the second invariant stress tensor. We consider in the constitutive equation (2.2.3) the case for which $\eta_\infty = 0$ and $\Gamma\dot{\gamma} < 1$ so we can write,

$$\tau = -\eta_0\left(1 + \Gamma\dot{\gamma}\right)\dot{\gamma} \tag{2.2.5}$$

The above model reduces to Newtonian for $\Gamma = 0$

The equations governing the flow in the wave frame of reference are

$$\frac{\partial u}{\partial x} + \frac{\partial v}{\partial y} = 0 \tag{2.2.6}$$

$$\rho\left(u\frac{\partial u}{\partial x} + v\frac{\partial u}{\partial y}\right) = -\frac{\partial p}{\partial x} - \frac{\partial \tau_{xx}}{\partial x} - \frac{\partial \tau_{yx}}{\partial y} - \left[\sigma B_0^2 + \frac{\eta_0}{k}\right](u + c) \tag{2.2.7}$$

$$\rho\left(u\frac{\partial v}{\partial x} + v\frac{\partial u}{\partial y}\right) = -\frac{\partial p}{\partial y} - \frac{\partial \tau_{xy}}{\partial x} - \frac{\partial \tau_{yy}}{\partial y} - \frac{\eta_0}{k}v \tag{2.2.8}$$

where ρ is the density, σ is the electrical conductivity and k is the permeability of the porous medium.

The corresponding dimensional boundary conditions are

$$u + \beta\tau_{xy} = -c \qquad \text{at} \qquad y = H(x) \text{ (slip condition)} \tag{2.2.9}$$

$$\frac{\partial u}{\partial y} = 0 \qquad \text{at} \qquad \text{y=0} \quad \text{(symmetry condition)} \tag{2.2.10}$$

Introducing the non-dimensional variables defined by

$$\bar{x} = \frac{x}{\lambda},\ \bar{y} = \frac{y}{a},\ \bar{u} = \frac{u}{c},\ \bar{v} = \frac{v}{c\delta},\ \delta = \frac{a}{\lambda},\ \bar{p} = \frac{pa^2}{\eta_0 c\lambda}, \phi = \frac{b}{a}$$

$$h = \frac{H}{a},\ \bar{t} = \frac{ct}{\lambda},\ \bar{\tau}_{xx} = \frac{\lambda}{\eta_0 c}\tau_{xx},\ \bar{\tau}_{xy} = \frac{a}{\eta_0 c}\tau_{xy},\ \bar{\tau}_{yy} = \frac{\lambda}{\eta_0 c}\tau_{yy},$$

$$\mathrm{R}_e = \frac{\rho ac}{\eta_0},\ We = \frac{\Gamma c}{a},\ \bar{\dot{\gamma}} = \frac{\dot{\gamma} a}{c},\ \bar{q} = \frac{q}{ac} \tag{2.2.11}$$

into the Equations (2.2.6) - (2.2.8), reduce to (after dropping the bars)

$$\frac{\partial u}{\partial x} + \frac{\partial v}{\partial y} = 0 \tag{2.2.12}$$

$$\mathrm{Re}\,\delta\left(u\frac{\partial u}{\partial x} + v\frac{\partial u}{\partial y}\right) = -\frac{\partial p}{\partial x} - \delta^2\frac{\partial \tau_{xx}}{\partial x} - \frac{\partial \tau_{xy}}{\partial y} - \left[M^2 + \frac{1}{Da}\right](u+1) \tag{2.2.13}$$

$$\mathrm{Re}\,\delta^3\left(u\frac{\partial v}{\partial x} + v\frac{\partial v}{\partial y}\right) = -\frac{\partial p}{\partial y} - \delta^2\frac{\partial \tau_{xy}}{\partial y} - \delta\frac{\partial \tau_{yy}}{\partial y} - \frac{\delta^2}{Da}v \tag{2.2.14}$$

where $\tau_{xx} = -2\left[1 + We\,\dot{\gamma}\right]\frac{\partial u}{\partial x}, \qquad \tau_{xy} = -\left[1 + We\,\dot{\gamma}\right]\left(\frac{\partial u}{\partial y} + \delta^2\frac{\partial v}{\partial x}\right),$

$\tau_{yy} = -2\delta\left[1 + We\,\dot{\gamma}\right]\frac{\partial v}{\partial y},$

$\dot{\gamma} = \left[2\delta^2\left(\frac{\partial u}{\partial x}\right)^2 + \left(\frac{\partial u}{\partial y} + \delta^2\frac{\partial v}{\partial x}\right)^2 + 2\delta^2\left(\frac{\partial v}{\partial y}\right)^2\right]^{\frac{1}{2}}$, $M = aB_0\sqrt{\frac{\sigma}{\eta_0}}$ is the Hartmann number and $Da = \frac{k}{a^2}$ is the Darcy number.

Under lubrication approach, neglecting the terms of order δ and Re, we get

$$\frac{\partial p}{\partial x}=\frac{\partial}{\partial y}\left\{\left[1+We\frac{\partial u}{\partial y}\right]\frac{\partial u}{\partial y}\right\}-\left[M^2+\frac{1}{Da}\right](u+1) \tag{2.2.15}$$

$$\frac{\partial p}{\partial y}=0 \tag{2.2.16}$$

From Eq. (2.2.15) and (2.2.16), we get

$$\frac{dp}{dx}=\frac{\partial^2 u}{\partial y^2}+We\frac{\partial}{\partial y}\left[\left(\frac{\partial u}{\partial y}\right)^2\right]-N^2(u+1) \tag{2.2.17}$$

here $N=\sqrt{M^2+\frac{1}{Da}}$.

The corresponding non-dimensional slip boundary conditions in the wave frame are given by

$$u+\beta\left[\frac{\partial u}{\partial y}+We\left(\frac{\partial u}{\partial y}\right)^2\right]=-1 \qquad \text{at} \qquad y=h=1+\phi\cos 2\pi x \tag{2.2.18}$$

$$\frac{\partial u}{\partial y}=0 \qquad \text{at} \qquad y=0 \tag{2.2.19}$$

The volume flow rate q in a wave frame of reference is given by

$$q=\int_0^h u dy\,. \tag{2.2.20}$$

The instantaneous flow $Q(X,t)$ in the laboratory frame is

$$Q(X,t)=\int_0^h U dY=\int_0^h (u+1)dy=q+h \tag{2.2.21}$$

The time averaged volume flow rate $\overline{Q}$ over one period $T\left(=\frac{\lambda}{c}\right)$ of the peristaltic wave is given by

$$\overline{Q}=\frac{1}{T}\int_0^T Q dt=q+1 \tag{2.2.22}$$

2.3 Solution

Since Eq. (2.2.17) is a non-linear differential equation, it is not possible to obtain closed form solution. Therefore we employ regular perturbation to find the solution.

For perturbation solution, we expand $u, \frac{dp}{dx}$ and q as follows

$$u = u_0 + We\,u_1 + O\left(We^2\right) \tag{2.3.1}$$

$$\frac{dp}{dx} = \frac{dp_0}{dx} + We\frac{dp_1}{dx} + O\left(We^2\right) \tag{2.3.2}$$

$$q = q_0 + We\,q_1 + O\left(We^2\right) \tag{2.3.3}$$

Substituting these equations into the Eqs. (2.2.17) - (2.2.19), we obtain

2.3.1. System of order We^0

$$\frac{\partial^2 u_0}{\partial y^2} - N^2 u_0 = \frac{dp_0}{dx} + N^2 \tag{2.3.4}$$

and the respective boundary conditions are

$$u_0 + \beta\frac{\partial u_0}{\partial y} = -1 \qquad \text{at} \qquad y = h \tag{2.3.5}$$

$$\frac{\partial u_0}{\partial y} = 0 \qquad \text{at} \qquad y = 0 \tag{2.3.6}$$

2.3.2. System of order We^1

$$\frac{\partial^2 u_1}{\partial y^2} - N^2 u_1 = \frac{dp_1}{dx} - \frac{\partial}{\partial y}\left[\left(\frac{\partial u_o}{\partial y}\right)^2\right] \tag{2.3.7}$$

and the respective boundary conditions are

$$u_1 + \beta\frac{\partial u_1}{\partial y} + \beta\left(\frac{\partial u_0}{\partial y}\right)^2 = 0 \quad \text{at} \qquad y = h \tag{2.3.8}$$

$$\frac{\partial u_1}{\partial y} = 0 \qquad \text{at} \qquad y = 0 \tag{2.3.9}$$

2.3.3 Solution for system of order We^0

Solving Eq. (3.4) using the boundary conditions (3.5) and (3.6), we obtain

$$u_0 = \frac{1}{N^2}\frac{dp_0}{dx}\left[\frac{\cosh Ny}{\cosh Nh + \beta N \sinh Nh} - 1\right] - 1 \tag{2.3.10}$$

The volume flow rate q_0 is given by

$$q_0 = \frac{dp_0}{dx}\frac{\left[\sinh Nh - Nh\left(\cosh Nh + \beta N \sinh Nh\right)\right]}{N^3\left(\cosh Nh + \beta N \sinh Nh\right)} - h \tag{2.3.11}$$

From Eq. (2.3.11), we have

$$\frac{dp_0}{dx} = \frac{N^3\left(q_0 + h\right)\left(\cosh Nh + \beta N \sinh Nh\right)}{\left[\sinh Nh - Nh\left(\cosh Nh + \beta N \sinh Nh\right)\right]} \tag{2.3.12}$$

2.3.4 Solution for system of order We^1

Substituting Eq. (2.3.10) in the Eq. (2.3.7) and solving the Eq. (2.3.7), using the boundary conditions (2.3.8) and (2.3.9), we obtain

$$u_1 = \frac{1}{N^2}\frac{dp_1}{dx}\left[\frac{\cosh Ny}{\left(\cosh Nh + \beta N \sinh Nh\right)} - 1\right] + \frac{2}{3}\frac{\left(\frac{dp_0}{dx}\right)^2}{N^3 A_1^3}\left[\begin{array}{l} A_2 \cosh Ny + \\ A_1 \sinh Ny - \frac{A_1}{2}\sinh 2Ny \end{array}\right] \tag{2.3.13}$$

Where $A_1 = \cosh Nh + \beta N \sinh Nh$

$$A_2 = -\sinh Nh + \frac{1}{2}\sinh 2Nh - \beta N \cosh Nh + N\beta \cosh 2Nh - \frac{3}{2}N\beta \sinh^2 Nh$$

The volume flow rate q_1 is given by

$$q_1 = \frac{1}{N^3 A_1}\frac{dp_1}{dx}\left[\sinh Nh - NhA_1\right] + \frac{2}{3}\frac{A_3}{N^4 A_1^3}\left(\frac{dp_0}{dx}\right)^2 \tag{2.3.14}$$

where $A_3 = A_2 \sinh Nh + A_1 \cosh Nh - \frac{A_1}{4}\cosh 2Nh - \frac{3}{4}A_1$.

From Eq. (2.3.14), we have

$$\frac{dp_1}{dx} = \frac{N^3\left[q_1 - \frac{2}{3}\frac{A_3}{N^4 A_1^3}\left(\frac{dp_0}{dx}\right)^2\right]A_1}{\left(\sinh Nh - NhA_1\right)} \tag{2.3.15}$$

Substituting Equations (2.3.12) and (3.15) into second equation of the Eq. (2.3.2) and using the relation $\frac{dp_0}{dx} = \frac{dp}{dx} - We\frac{dp_1}{dx}$ and neglecting terms greater than $O(We)$, we get

$$\frac{dp}{dx} = \left[\frac{(q+h)N^3 A_1}{(\sinh Nh - NhA_1)} - We\frac{2N^5 A_3 (q+h)^2}{3(\sinh Nh - NhA_1)^3} \right] \tag{2.3.16}$$

The dimensionless pressure rise per one wavelength in the wave frame is defined as

$$\Delta p = \int_0^1 \frac{dp}{dx} dx \tag{2.3.17}$$

Note that, as $Da \to \infty$ and $\beta \to 0$ our results coincide with the results of Subba Reddy et al. (2011).

2.4. Results and Discussions

Fig. 2.2 shows the variation of axial pressure gradient $\frac{dp}{dx}$ with Weissenberg number We for $\phi = 0.6$, $M = 1$, $\beta = 0.1$ and $Da = 0.1$. It is observed that, the axial pressure gradient $\frac{dp}{dx}$ increases with increasing Weissenberg number We.

The variation of axial pressure gradient $\frac{dp}{dx}$ with slip parameter β for $\phi = 0.6$, $M = 1$, $We = 0.02$ and $Da = 0.1$ is shown in Fig. 2.3. It is found that, the axial pressure gradient $\frac{dp}{dx}$ decreases with increasing slip parameter β.

Fig. 2.4 depicts the variation of axial pressure gradient $\frac{dp}{dx}$ with Hartmann number M for $\phi = 0.6$, $Da = 0.1, \beta = 0.1$ and $We = 0.02$. It is noted that, the axial pressure gradient $\frac{dp}{dx}$ increases with increasing Hartmann number M.

The variation of axial pressure gradient $\frac{dp}{dx}$ with Darcy number Da for $\phi = 0.6$, $M = 1, \beta = 0.1$ and $We = 0.02$ is depicted in Fig. 2.5. It is observed that, the axial pressure gradient $\frac{dp}{dx}$ decreases with increasing Darcy number Da.

Fig. 2.6 illustrates the variation of axial pressure gradient $\frac{dp}{dx}$ with amplitude ratio ϕ for $M = 1, Da = 0.1$, $\beta = 0.1$ and $We = 0.02$. It is found that, the axial pressure gradient $\frac{dp}{dx}$ increases with increasing amplitude ratio ϕ.

The variation of pressure rise Δp with time-averaged volume flow rate $\overline{Q}$ for different values of Weissenberg number We with $\phi = 0.6$, $M = 1, \beta = 0.1$ and $Da = 0.1$ is shown in Fig. 2.7. It is noted that, the time averaged volume flow rate $\overline{Q}$ increases with increasing We in pumping $(\Delta p > 0)$, free-pumping $(\Delta p = 0)$ and co-pumping $(\Delta p < 0)$ regions. Further, it is observed that, the pumping is more for Williamson fluid than that of Newtonian fluid.

Fig. 2.8 shows the variation of pressure rise Δp with time-averaged volume flow rate $\overline{Q}$ for different values of slip parameter β with $\phi = 0.6$, $M = 1$, $We = 0.02$ and $Da = 0.1$. It is observed that, the time-averaged volume flow rate $\overline{Q}$ decreases with increasing β in both the pumping and free pumping regions, while it increases with increasing β in co-pumping region for chosen $\Delta p(< 0)$.

The variation of pressure rise Δp with time-averaged volume flow rate $\overline{Q}$ for different values of Hartmann number M with $\phi = 0.6$, $Da = 0.1$, $\beta = 0.1$ and

$We = 0.02$ is shown in Fig. 2.9. It is found that, the time-averaged volume flow rate $\overline{Q}$ increases with increasing M in the pumping region, while it decreases with increasing M in both the free-pumping and co-pumping regions.

Fig. 2.10 depicts the variation of pressure rise Δp with time-averaged volume flow rate $\overline{Q}$ for different values of Darcy number Da with $\phi = 0.6$, $M = 1$, $\beta = 0.1$ and $We = 0.02$. It is found that, the time-averaged volume flow rate $\overline{Q}$ decreases with increasing Da in the pumping region, while it increases with increasing Da in both the free-pumping and co-pumping regions.

The variation of pressure rise Δp with time-averaged volume flow rate $\overline{Q}$ for different values of amplitude ratio ϕ with $We = 0.02$, $M = 1, \beta = 0.1$ and $Da = 0.1$ is depicted in Fig. 2.11. It is observed that, the time-averaged volume flow rate $\overline{Q}$ increases with increasing ϕ in both the pumping and free-pumping regions, while it decreases with increasing ϕ in the co-pumping region for chosen $\Delta p(<0)$.

2.5. Conclusions

In this chapter, we investigated the effect of slip on the peristaltic flow of a Williamson fluid through a porous medium in a planar channel, under the assumptions of low Reynolds number and long wavelength. The perturbation series in the Weissenberg number ($We < 1$) was used to obtain explicit forms for velocity field, pressure gradient per one wavelength. It is found that, the axial pressure gradient increases with increasing We, M and ϕ, while it decreases with increasing β and Da. Further, it is observed that in the pumping region the time averaged flow rate $\overline{Q}$ increases with increasing with increasing We, M and ϕ, while it decreases with increasing β and Da. Moreover it is found that the pumping is more for Williamson fluid than that of Newtonian fluid.

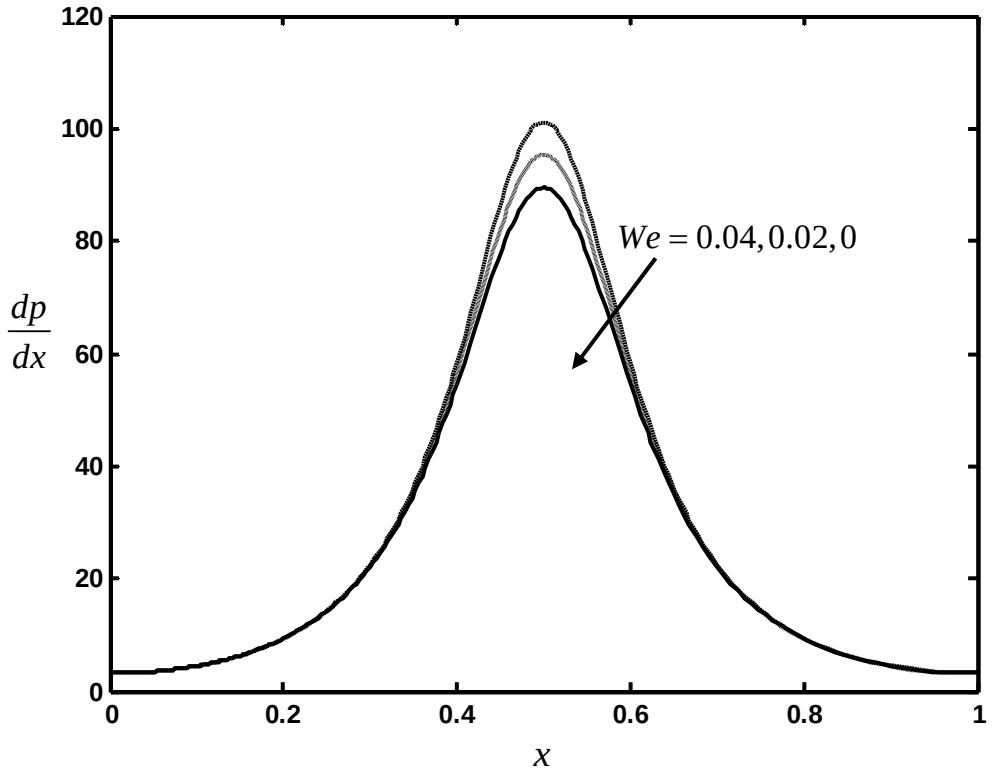

Fig. 2.2 The variation of axial pressure gradient $\frac{dp}{dx}$ with We for $\phi = 0.6$, $M = 1$, $\beta = 0.1$ and $Da = 0.1$.

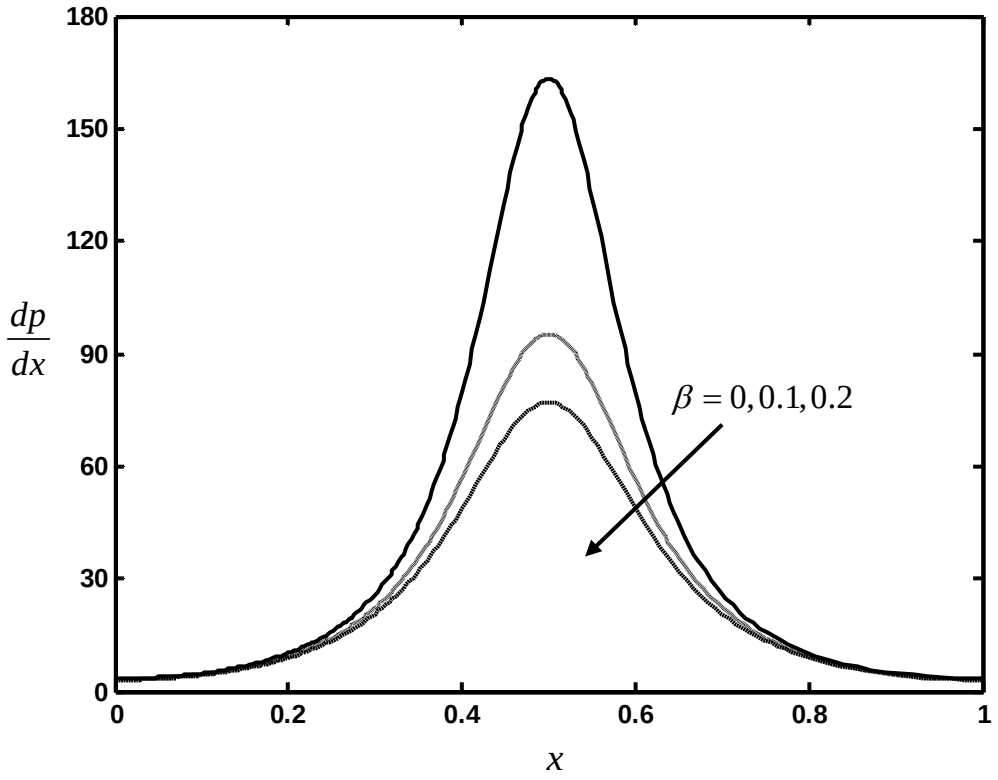

Fig. 2.3 The variation of axial pressure gradient $\frac{dp}{dx}$ with β for $\phi = 0.6$, $M = 1$, $We = 0.02$ and $Da = 0.1$.

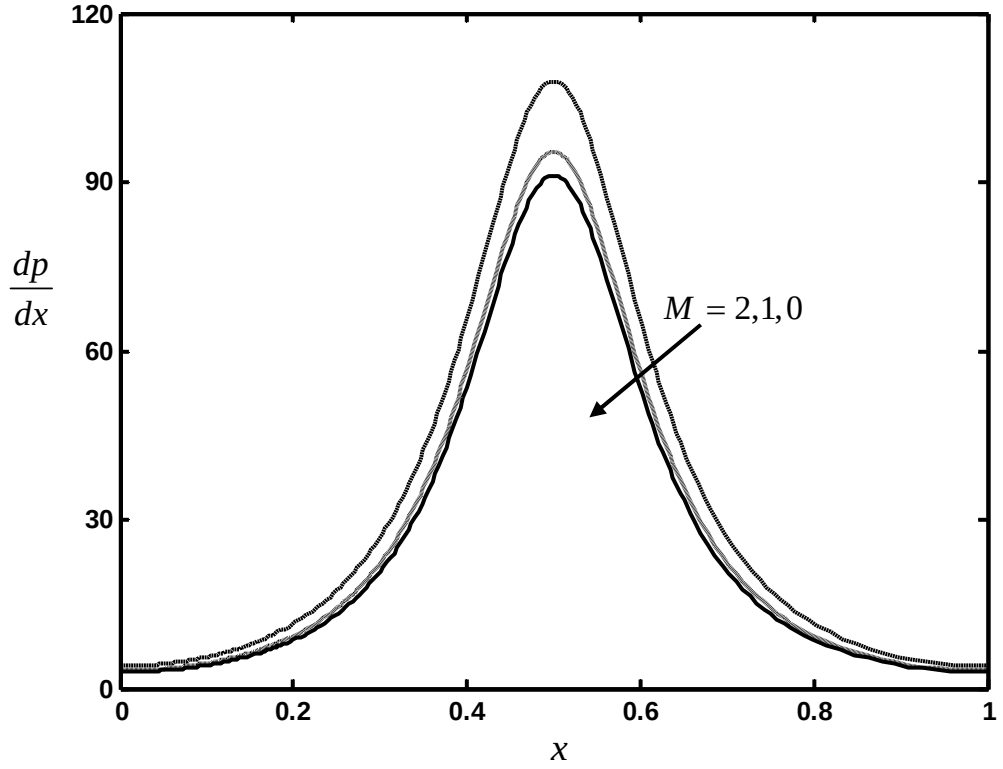

Fig. 2.4 The variation of axial pressure gradient $\frac{dp}{dx}$ with M for $\phi = 0.6$, $\beta = 0.1$, $We = 0.02$ and $Da = 0.1$.

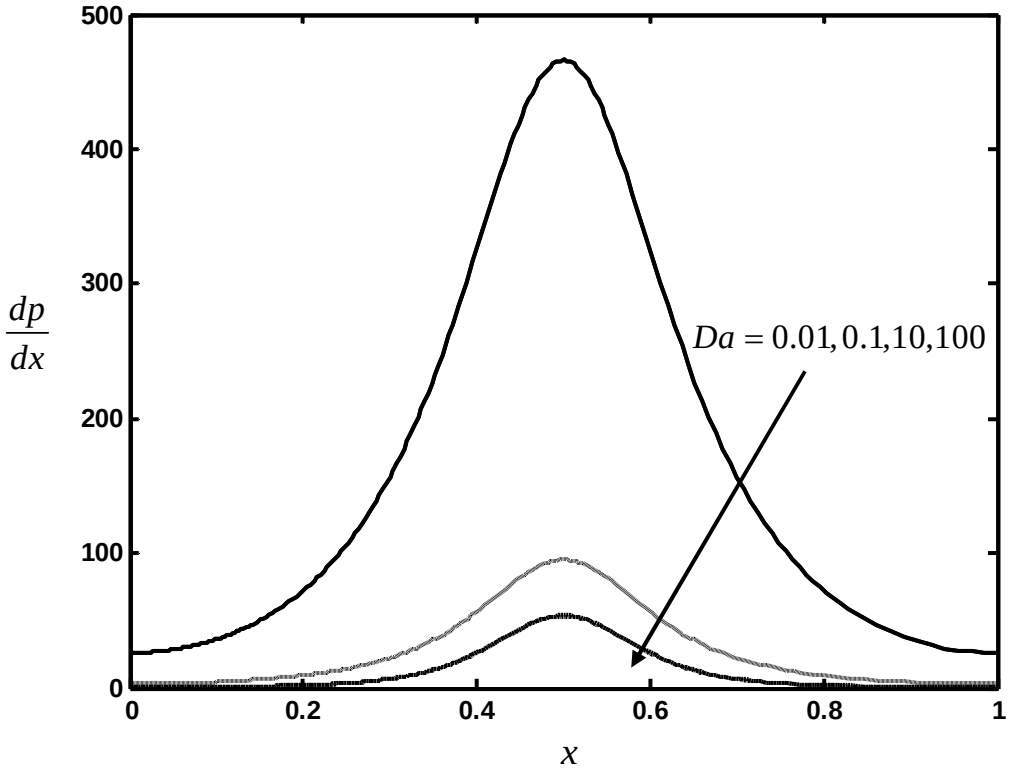

Fig. 2.5 The variation of axial pressure gradient $\frac{dp}{dx}$ with Da for $\phi = 0.6$, $M = 1$, $\beta = 0.1$ and $We = 0.02$.

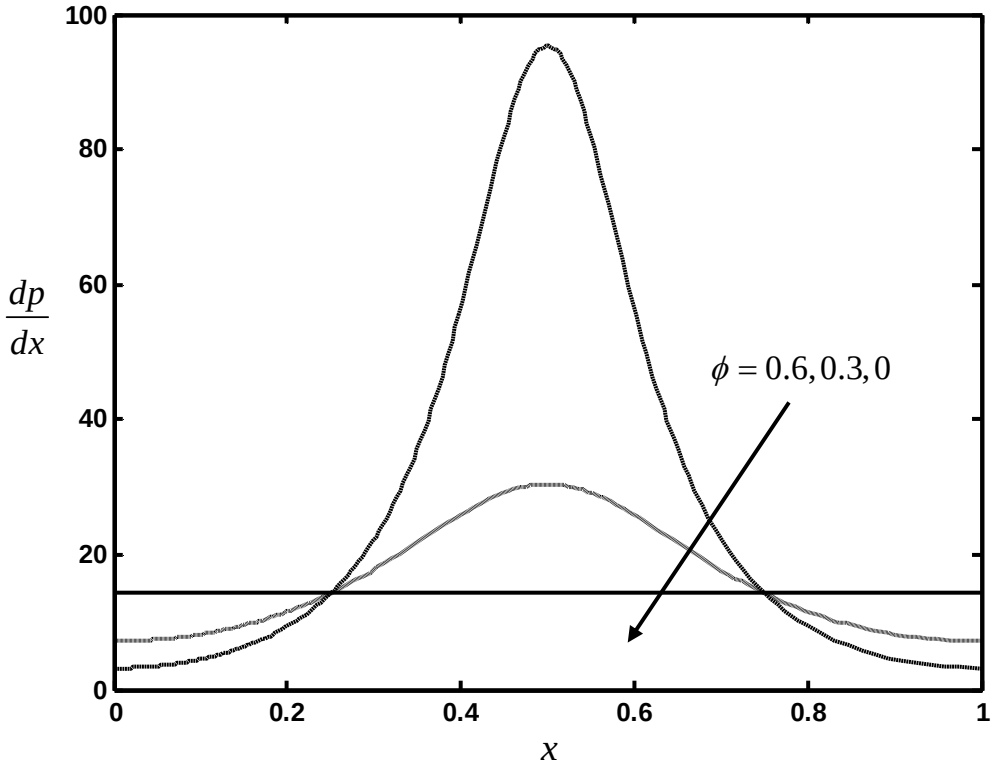

Fig. 2.6 The variation of axial pressure gradient $\frac{dp}{dx}$ with ϕ for $Da = 0.1$, $M = 1$, $\beta = 0.1$ and $We = 0.02$.

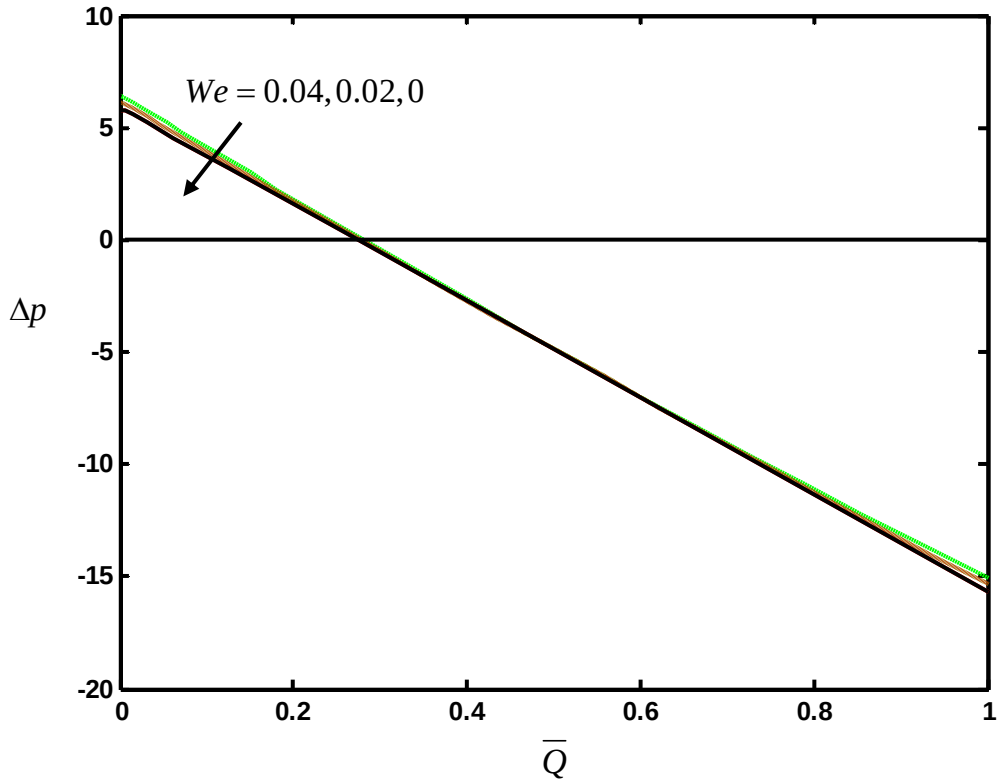

Fig. 2.7 The variation of pressure rise Δp with time-averaged volume flow rate $\overline{Q}$ for different values of We with $\phi = 0.6$, $M = 1$, $\beta = 0.1$ and $Da = 0.1$.

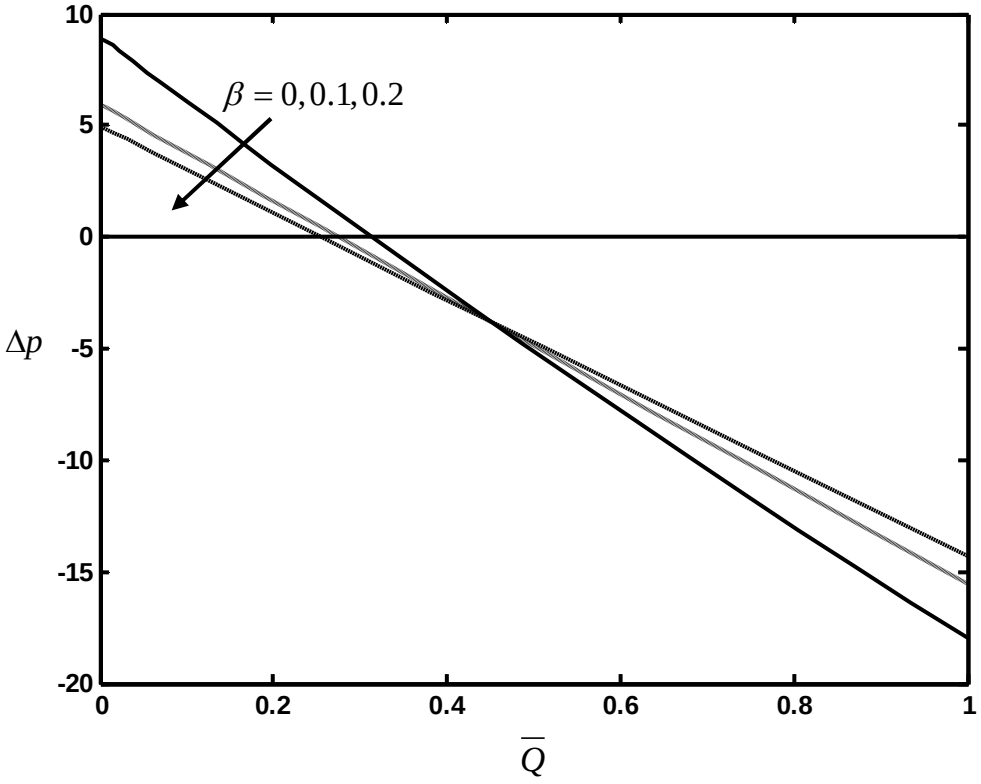

Fig. 2.8 The variation of pressure rise Δp with time-averaged volume flow rate $\overline{Q}$ for different values of β with $\phi = 0.6$, $M = 1$, $We = 0.02$ and $Da = 0.1$.

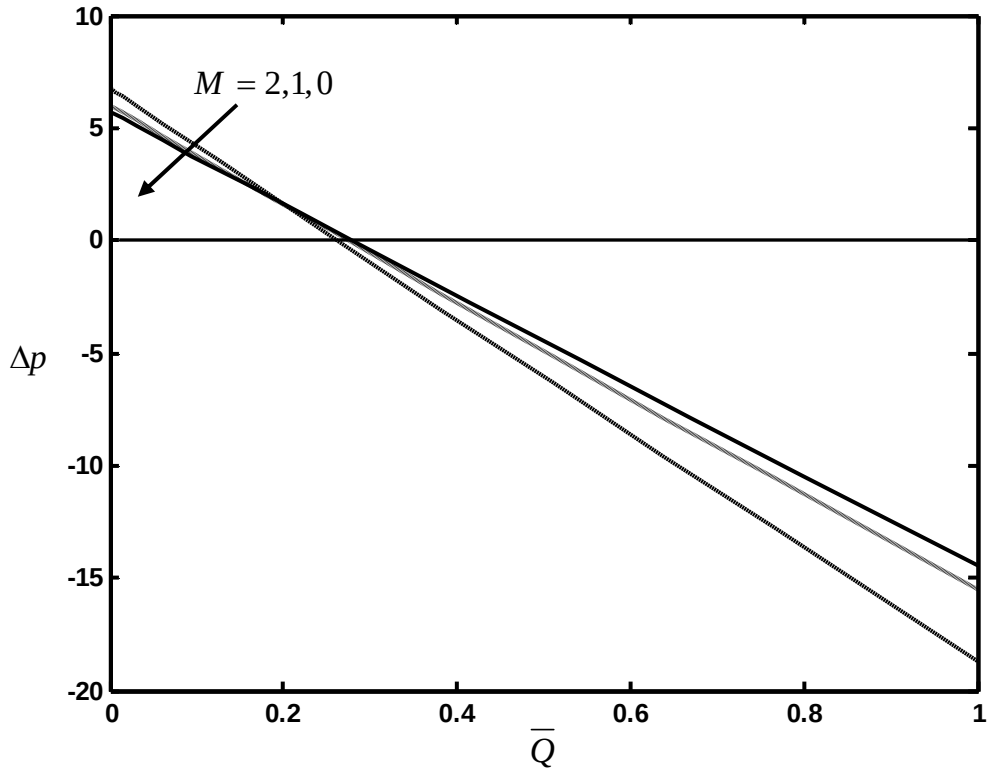

Fig. 2.9 The variation of pressure rise Δp with time-averaged volume flow rate $\overline{Q}$ for different values of M with $\phi = 0.6$, $\beta = 0.1$, $We = 0.02$ and $Da = 0.1$.

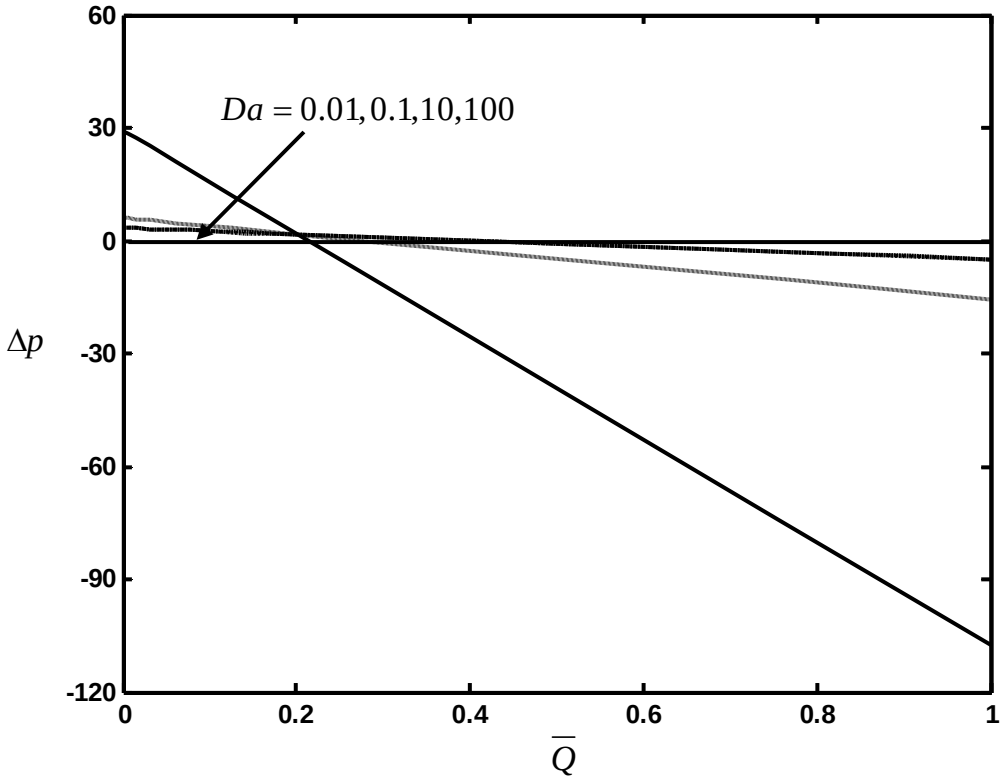

Fig. 2.10 The variation of pressure rise Δp with time-averaged volume flow rate $\overline{Q}$ for different values of Da with $\phi = 0.6$, $M = 1$, $\beta = 0.1$ and $We = 0.02$.

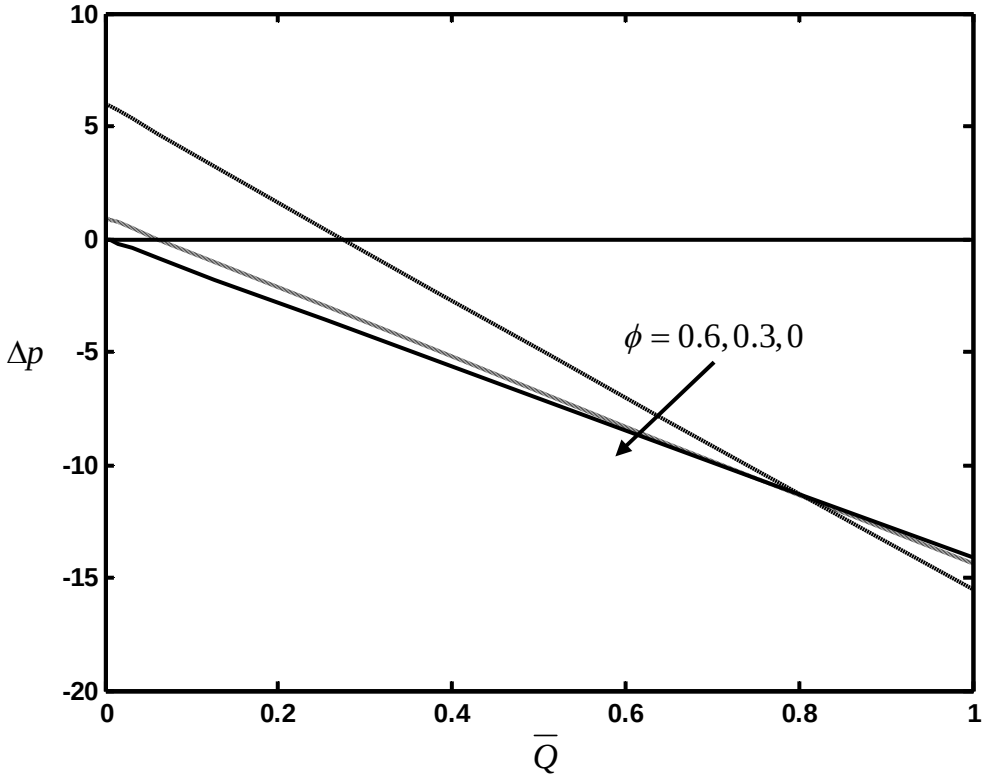

Fig. 2.11 The variation of pressure rise Δp with time-averaged volume flow rate $\overline{Q}$ for different values of ϕ with $We = 0.02$, $M = 1$, $\beta = 0.1$ and $Da = 0.1$.